ORGANOMETALLICS

Article

pubs.acs.org/Organometallics

Solvent Effects on Hydride Transfer from Cp*(P-P)FeH to BNA$^+$ Cation

Fanjun Zhang, Xin Xu, Yingjie Zhao, Jiong Jia, Chen-Ho Tung, and Wenguang Wang*

School of Chemistry and Chemical Engineering, Shandong University, No. 27 South Shanda Road, Jinan 250100, China

Supporting Information

ABSTRACT: Examining of the hydride transfer reaction between Cp*($Ph_2PN^{tBu}PPh_2$)-FeH ($Ph_2PN^{tBu}PPh_2$ = *N*,*N*-bis(diphenylphosphanyl)*tert*-butylamine, **1-H**) and 1-benzyl-3-carbamoylpyridinium cation (BNA$^+$) in different solvents, we found that the solvents exert considerable influence on the hydride transfer processes. A coordinating solvent molecule such as MeCN is not only a ligand which stabilizes the organo-iron fragment producing [Cp*($Ph_2PN^{tBu}PPh_2$)Fe(NCMe)]$^+$ ([**1**(NCMe)]$^+$), but also assists the hydride transfer. In THF, reaction of **1-H** with BNA$^+$ under high pressure of nitrogen (60 psi) giving the iron(II)−nitrogen complex [Cp*($Ph_2PN^{tBu}PPh_2$)Fe(N_2)]$^+$ ([**1**-N_2]$^+$) and BNAH. In CH_2Cl_2, [**1**-N_2]$^+$ catalyzes the conversion of **1-H** to Cp*($Ph_2PN^{tBu}PPh_2$)-FeCl (**1-Cl**), which hampers the expected hydride transfer reaction. In the presence of MeCN, the hydride transfer process in THF, CH_2Cl_2, or benzene was achieved affording the reduced BNAH and [**1**(NCMe)]$^+$. New iron complexes in the [Cp*($Ph_2PN^{tBu}PPh_2$)-FeX]$^{n+}$ series (where n = 0, X = H or Cl; n = 1, X = MeCN, N_2, or Cl$^-$) were obtained and well characterized.

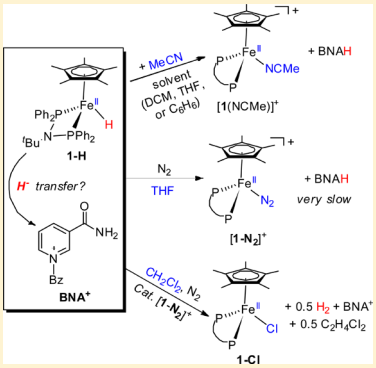

INTRODUCTION

The coenzyme nicotinamide adenine dinucleotide (phosphate) (NAD(P)H) provides electrons or energy for carbohydrate synthesis in the dark reactions of photosynthesis,[1] and in the preparation of nitrogen-containing heterocycles.[2] Reduction of pyridinium cations to the corresponding dihydropyridine is interesting and important,[3] not only because of its relevance to energy storage and release in the biological system but also because dihydropyridine derivatives are widely used as reductants in organocatalysis.[4] Intensive studies have focused on noble-metal hydrides such as Rh(III),[5] Ir(III),[4c,5c,6] Ru(II),[7] and Re(I),[7d] employed as hydride donors to reduce pyridinium cations. Mechanistic insights into factors that determine the regioselectivity of dihydropyridine products (1,4-isomer vs 1,6-isomer) have attracted particular attention (Scheme 1).

For example, the regioselective reduction of 1-benzyl-3-carbamoylpyridinium cation (BNA$^+$) to the 1,4-BNAH product was thought to proceed through a coordinative intermediate, in which the carbamoyl group in BNA$^+$ interacts with the metal center.[5a,b] Ishitani et al. reported such interactions in the case of BNA$^+$ and [(tpy)(bpy)RuH]$^+$ evidenced by spectroscopic studies.[7d] For pyridinium cations with a noncoordinating group such as −CF_3 or H at the C3 position, the corresponding 1,4-dihydropyridine products were proposed to coordinate with the Ru(II) center in a η^2 mode through a C=C bond at the initial formation stage.[7b] On the basis of the investigation of reducing iminium[8] and *N*-acylpyridinium cations by Cp(P-P)RuH hydrides, in which P-P = chelating diphosphine,[5c,9] Norton et al. suggested "a single-step H$^-$ transfer" mechanism to form the 1,2-product, and "a two-step e$^-$/H$^\bullet$ process" for only the 1,4-product.

Recently, we reported reduction of a range of *N*-benzylpyridinium cation derivatives by Cp*(P-P)FeH (P-P = bis(diphenylphosphino)methane (dppm), bis(diphenylphosphino)ethane (dppe), bis(diphenylphosphino)benzene (dppbz), or 1,2-bis(dicyclohexylphosphino)ethane (dcpe)). Our studies indicated that the *N*-benzylpyridinium cation is favorably reduced at the C6 position, affording the 1,6-isomer as the kinetically controlled product. The stability of the 1,6-products is very dependent on the substituent (R_2) at the C3 position. The results obtained suggested that H$^-$ transfer is more likely to be charge controlled, which is consistent with the "a single-step H$^-$ transfer" mechanism.[10] Unlike the systems based on the noble metal hydrides,[5c,9] the hydride transfer reaction between Cp*(P-P)FeH and pyridinium cations requires the coordinating solvent MeCN. The presence of MeCN seems not only to stabilize the organoiron products in the [Cp*(P-P)Fe(NCMe)]$^+$ form, but also affect significantly the hydride transfer process.

Scheme 1. Reduction of Pyridinium Cations to 1,6- and 1,4-Dihydropyridines by Metal Hydrides (M−H)

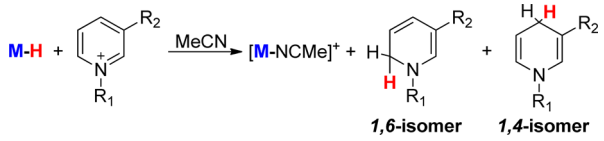

Received: December 7, 2016

DOI: 10.1021/acs.organomet.6b00907
Organometallics XXXX, XXX, XXX−XXX

In this paper, we examine the reactions between BNA^+ and **1-H** in various solvents such as CH_2Cl_2, THF, and benzene in the presence or absence of MeCN (Scheme 2). We found the

Scheme 2. Reactions of Cp*($Ph_2PN^{tBu}PPh_2$)FeH with BNA^+ in Different Solvents

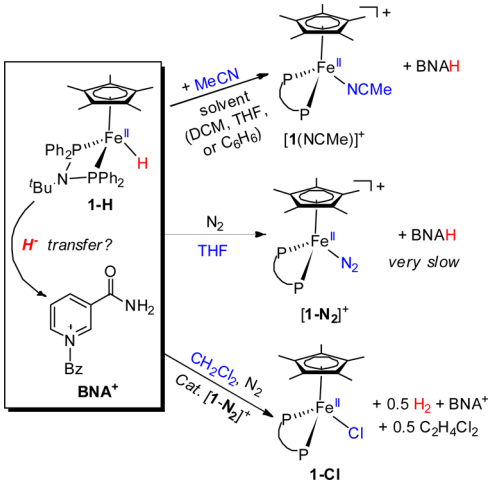

solvents exert an influence on such hydride transfer processes, beyond the rate of the hydride transfer and some side reactions that hamper the expected reduction of the BNA^+ cation. Besides **1-H** and $[\mathbf{1}(NCMe)]^+$, several new iron complexes $[\mathbf{1}\text{-}N_2]^+$, **1-Cl**, and $[\mathbf{1}\text{-}Cl]^+$ were isolated and characterized from these reactions.

RESULTS AND DISCUSSION

Synthesis and Characterization. Compound **1-H** was synthesized according to the reported procedure for Cp*(P-P)FeH,[10] using the acetonitrile complex $[\mathbf{1}(NCMe)]^+$ as the precursor. Treatment of $[\mathbf{1}(NCMe)]^+$ with $NaBH_4$ in THF leads to gradual color changes from dark red to orange. The product was recrystallized from pentane, and isolated by filtration in a yield of 78%. The ^1H NMR spectrum of **1-H** displays its hydride resonance at −13.5 ppm (J_{P-H} = 63 Hz) as a triplet.

Crystals of **1-H** suitable for X-ray diffraction were obtained by cooling the saturated pentane solution to −30 °C. The structure of **1-H** was confirmed crystallographically, and the hydride ligand was located (Figure 1). The framework Cp*(P-P)FeX is similar to the Cp*(P-P)FeH series described previously.[10] The bite angle ∠P−Fe−P in **1-H** is 72.72(2)°, 2.6° smaller than that in Cp*(dppm)FeH (75.33°). It has been suggested that the bite angle in Cp*(P-P)MX compounds reflects the steric hindrance around the metal center.[8b] Compared with the Cp*(P-P)FeH (P-P = dppm, dppe, dppbz, or dcpe),[10] **1-H** exhibits the smallest bite angle.

The cyclic voltammogram of **1-H** exhibits a one-electron reversible oxidation process at −0.29 V vs $Fc^{+/0}$ for the $[\mathbf{1}\text{-}H]^{+/0}$ couple. Compared to Cp*(dppm)FeH, the oxidation potential of **1-H** is 60 mV less negative, which indicates that dppm has better electron-donating properties than the $Ph_2PN^{tBu}PPh_2$ ligand for the Cp*FeH motif. For the reduction of BNA^+ or relative organocations, Cheng et al. suggested that a multistep mechanism ($e^-/H^\bullet$ or $e^-/H^+/e^-$) would be followed if the energy gap (ΔG_{ET}) of the initial electron transfer process (ET) between the cations and the reducing substrate is considerably smaller than the empirical

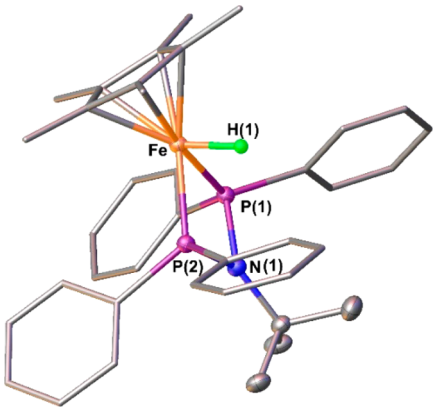

Figure 1. Structure (50% probability thermal ellipsoids) of **1-H**. For clarity, the Cp* ring and phenyl groups are drawn as lines. Hydrogen atoms with the exception of the hydride ligand are omitted. Selected distances (Å) and angles (deg): Fe−P(1) 2.1169(5), Fe−P(2) 2.1320(5), and P(1)−Fe−P(2) 72.72(2).

critical limit of 1.0 eV.[11] On the basis of the reduction potential of BNA^+ (−1.5 V vs $Fc^{+/0}$), ΔG_{ET} for the electron transfer process for **1-H** was calculated to be 1.21 eV and accordingly, the initial ET from **1-H** to BNA^+ would appear to be thermodynamically unfavorable.

Hydride Transfer in THF. The reaction of **1-H** with BNA^+ was examined in THF, which was found to be weakly coordinating solvent for $[Cp^*(P\text{-}P)Fe]^+$ species.[12] To assist BNA^+ dissolving well in THF, we exchanged the counterion, replacing PF_6^- with BPh_4^- (tetraphenylborate). The stoichiometric reaction of **1-H** and $[BNA]BPh_4$ (0.04 M) in THF-d_8 was conducted in a J. Young tube at room temperature. After 24 h, the reaction mixture was analyzed by NMR at room temperature. The peaks were broadened in the ^1H NMR spectrum, and the hydride signal for **1-H** at −13.5 ppm was absent. The ^{31}P NMR spectrum exhibited a new signal at 114.9 ppm, and the phosphorus signals for **1-H** were not observed. However, upon cooling down the reaction solution to −20 °C, both the hydride and phosphorus signals for **1-H** appeared as broad peaks in the ^1H and ^{31}P NMR spectra. At −60 °C, the ^1H NMR spectrum features a triplet signal at −13.5 ppm (J_{P-H} = 63 Hz) corresponding to the ^{31}P NMR signal at δ 128.4 for **1-H**. As shown in Figure 2, we recorded the ^{31}P NMR spectra at various temperatures from 20 °C to −60 °C. Besides the ^{31}P signal for **1-H**, a new signal at 114.9 ppm was also observed, indicating the production of a new organo-iron species.

$$[Fe^{II}\text{−}H]^0 + BNA^+ + N_2 \rightarrow [Fe^{II}\text{−}N_2]^+ + BNAH \qquad (1)$$

This new species was thought to be $[\mathbf{1}\text{-}N_2]^+$. To prove this hypothesis (eq 1), we conducted the reaction of **1-H** and BNA^+ in THF under higher pressure (60 psi) of nitrogen at room temperature. After 48 h, **1-H** was almost completely converted to $[\mathbf{1}\text{-}N_2]^+$, which was isolated and further characterized (eq 1). In the IR spectrum, $[\mathbf{1}\text{-}N_2]^+$ exhibits a strong ν_{NN} band at 2132 cm^{-1}, which is close to the N−N stretching frequency of 2130 cm^{-1} for $[HFe(dppe)_2(N_2)]BPh_4$,[13] but much higher than that for $[\{CpFe(dppe)\}_2(N_2)]^{2+}$ (2040 cm^{-1}),[14] in which N_2 is as a bridging ligand coordinated to the two metals.

The structure of $[\mathbf{1}\text{-}N_2]BPh_4$ was confirmed by X-ray crystallography (Figure 3). In the $[\mathbf{1}\text{-}N_2]^+$ cation, N_2 is

DOI: 10.1021/acs.organomet.6b00907
Organometallics XXXX, XXX, XXX−XXX

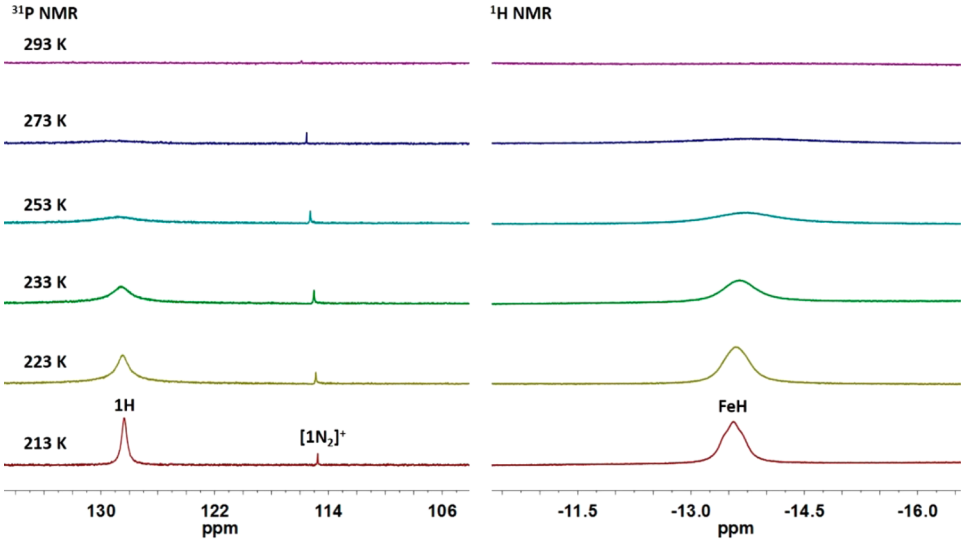

Figure 2. ^{31}P NMR (left) and ^{1}H NMR (right, hydride region) spectra recorded for the reaction of **1-H** and BNA^+ in THF-d_8 at various temperatures from 293 to 213 K.

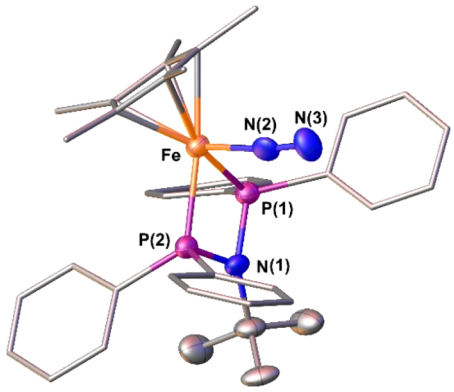

Figure 3. Structure (50% probability thermal ellipsoids) of $[\mathbf{1}\text{-}N_2]^+$. For clarity, the four phenyl groups bound to phosphorus are drawn as lines and hydrogen atoms are omitted. Selected distances (Å) and angles (deg): Fe−N(2) 1.833(9), N(2)−N(3) 1.12(1), Fe−P(1) 2.210(3), Fe−P(2) 2.233(3), P(1)−Fe−P(2) 70.9(1), and Fe−N(2)−N(3) 173.4(8).

unambiguously coordinated to the iron(II) center in an end-on binding mode.[15] The N−N bond distance 1.12(1) Å is comparable to 1.13 Å observed for $[Cp(dippe)Fe(N_2)]^+$ (dippe =1,2-bis(diisopropylphosphino)ethane).[16] Compared to $[Cp(dippe)Fe(N_2)]^+$, the Fe−N distance 1.833(9) Å is about 0.07 Å longer, while the Fe−N−N angle 173.4(8)° is almost unchanged. Combined with the N−N stretching frequency, these crystallographic data for $[\mathbf{1}\text{-}N_2]^+$ indicate that the N_2 molecule was activated minimally at the iron center.

The N_2 ligand in $[\mathbf{1}\text{-}N_2]^+$ is very labile, and can be replaced by CO or MeCN affording $[Cp^*(Ph_2PN^{tBu}PPh_2)Fe(CO)]^+$ (Figures S10 and S11 of the Supporting Information) and $[\mathbf{1}(NCMe)]^+$ respectively. Especially, the reaction of $[\mathbf{1}\text{-}N_2]^+$ with Cp*(dcpe)FeH in THF gave **1-H** and 16-electron cationic complex $[Cp^*(dcpe)Fe]^+$, which is stable toward N_2. The structure of $[Cp^*(dcpe)Fe]^+$ was established by single-crystal X-ray diffraction (Figure S25).

For the reaction of **1-H** and BNA^+ in THF, variable-temperature ^{31}P NMR spectra showing coalescences and decoalescences probably belong to the intermolecular interaction between the unreacted **1-H** and the organo-iron product $[\mathbf{1}\text{-}N_2]^+$ (eq 2). Such interaction were also observed for the THF solutions of **1-H** and $[\mathbf{1}\text{-}N_2]^+$ (20 mol %) in the independent NMR experiments (Figure S12). It should be noticed that the NMR spectra of **1-H** recorded in THF features the distinguishable signals for the hydride and the diphosphines ligands.

$$[Fe^{II}\text{−}N_2]^+ + *[Fe^{II}\text{−}H]^0 \rightarrow [Fe^{II}\text{−}H]^0 + *[Fe^{II}\text{−}N_2]^+ \quad (2)$$

Norton et al. reported the formation of bimetallic bridging hydride complex $\{[Cp^*(2\text{-}(2\text{-pyridyl})phenyl)Rh]_2(\mu\text{-}H)\}^+$ by the reaction of Cp*(2-(2-pyridyl)phenyl)RhH and $[Cp^*(2\text{-}(2\text{-pyridyl})phenyl)Rh(NCMe)]^+$ in C_6H_6.[17] Dissolving the bridging hydride complex in MeCN resulted in the recovery of Cp*(2-(2-pyridyl)phenyl)RhH and $[Cp^*(2\text{-}(2\text{-pyridyl})phenyl)Rh(NCMe)]^+$. The related bimetallic complex, $\{[Cp^*(CO)_2Ru]_2(\mu\text{-}H)\}^+$ was proposed as an intermediate in the reduction of $[Ph_3C]BF_4$ by $Cp^*(CO)_2RuH$ by Bullock.[18] Owing to the lability of the N_2 ligand, the equilibrium between $[\mathbf{1}\text{-}N_2]^+$ and the 16-electron cation complex $[Cp^*(Ph_2PN^{tBu}PPh_2)Fe]^+$ and N_2 is possible. The hydride abstraction from **1-H** by $[Cp^*(Ph_2PN^{tBu}PPh_2)Fe]^+$ can be through an intermediate of $[Fe^{II}\text{−}H\text{−}Fe^{II}]^+$ (unobserved) species.

Hydride Transfer in THF in the Presence of MeCN. When the reaction of **1-H** with BNA^+ was performed in THF-d_8 in the presence of 10 equiv of MeCN, stoichiometric hydride transfer proceeded and produced $[\mathbf{1}(NCMe)]^+$ and BNAH as both 1,6- and 1,4-isomers (eq 3).

$$\mathbf{1\text{-}H} + BNA^+ + MeCN \rightarrow [1(NCMe)]^+ + 1,6\text{-BNAH} + 1,4\text{-BNAH} \quad (3)$$

The reaction of **1-H** with excess BNA^+ (10 equiv) in THF-d_8/CD_3CN (2/1) was monitored by ^1H NMR at 298 K, giving a pseudo-first-order rate constant k_{obs}. Variation of $[BNA^+]$ from 0.146 to 0.379 M showed that k_{obs} for **1-H** was linearly related to $[BNA^+]$, indicating that hydride transfer from **1-H** to BNA^+ is a second order reaction,[8b] and the rate

DOI: 10.1021/acs.organomet.6b00907
Organometallics XXXX, XXX, XXX−XXX

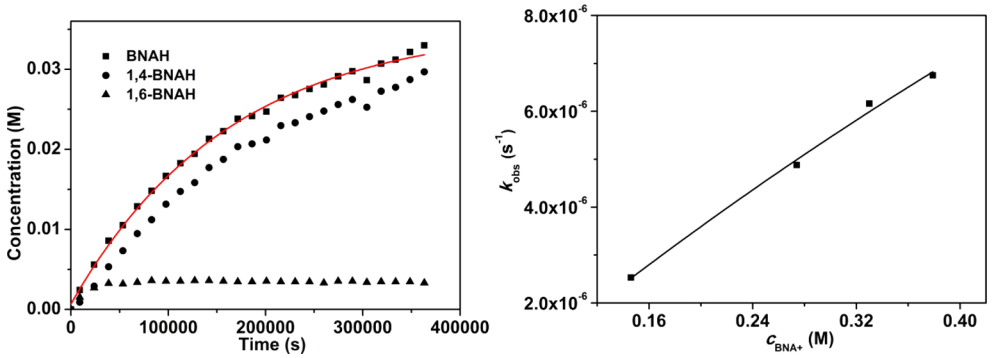

Figure 4. Left, concentrations of BNAH, 1,4-BNAH and 1,6-BNAH over time during the reaction of **1-H** with BNA^+ in THF-d_8/CD_3CN (2/1) at 298 K. The initial [**1-H**] and [BNA^+] are 3.30×10^{-2} M and 3.30×10^{-1} M, respectively. Results: $k_{obs} = 6.2(3) \times 10^{-6}$ s^{-1}, $R^2 = 0.997$. Right, plot of k_{obs} vs [BNA^+] for the reaction of **1-H** with BNA^+. Results: $k = 1.9(1) \times 10^{-5}$ M^{-1} s^{-1}, $R^2 = 0.992$.

constant k was determined to be $1.9(1) \times 10^{-5}$ M^{-1} s^{-1} (Figure 4).

The MeCN in the hydride transfer from Cp*(P-P)FeH (Fe^{II}–H) to BNA^+ could behave as (i) a ligand stabilizing the organo iron(II) fragment after the reaction, or (ii) a nucleophilic agent giving impetus to the hydride transfer. In principle, there are two possible pathways for "a single-step H^- transfer" mechanism. One is Fe^{II}–H attacking the C6 position of BNA^+ nucleophilically, affording BNAH and the 16 e^- unsaturated [Cp*(P-P)Fe]$^+$ species ([Fe^{II}]$^+$), which was trapped by MeCN, producing [Cp*(P-P)Fe(NCMe)]$^+$ ([Fe^{II}–NCMe]$^+$, eqs 4 and 5)

$$[Fe^{II}–H]^0 + BNA^+ \rightarrow [Fe^{II}]^+ + BNAH \quad (4)$$

$$[Fe^{II}]^+ + MeCN \rightarrow [Fe^{II}–NCMe]^+ \quad (5)$$

The other possible pathway could involve an intermediate of [Fe^{II}–H---BNA]$^+$ arising from the weak static interaction between Fe^{II}—H and BNA^+. Coordinative molecules such as MeCN or N_2 attacks the iron center of [Fe^{II}–H---BNA]$^+$ driving the hydride transfer (eq 6).

$$[Fe^{II}–H]^0 + BNA^+ + MeCN \rightarrow [Fe^{II}–NCMe]^+ + BNAH \quad (6)$$

To understand the behavior of MeCN in the hydride transfer process, we examined the reaction of **1-H** with BNA^+ in CD_2Cl_2 and C_6D_6 in the presence of MeCN.

Hydride Transfer in CH_2Cl_2. It has been reported that the hydride transfer from $Cp^*(CO)_2FeH$ to $[Ph_3C]BF_4$ in CH_2Cl_2 produced Ph_3CH and [$Cp^*(CO)_2Fe$–F–BF_3].[18] For the reaction of **1-H** with BNA^+ in CD_2Cl_2, the color of the solution turned to dark green after 24 h, and the NMR spectral analysis suggest the reaction mixture is paramagnetic. By contrast, **1-H** is very stable toward CH_2Cl_2 in solution under a N_2 atmosphere. At least in 48 h there was no reaction observed, judging from ^{31}P and ^1H NMR studies.

To understand precisely the reactions that occur, we conducted the reaction in a larger scale in CH_2Cl_2 using 50 mg **1-H** (0.079 mmol) and 1 equiv [BNA]BPh_4. After 36 h, the solvent was removed under vacuum and the residue was extracted with hexane. The dark green compound dissolves readily in hexane, and the undissolved white solid was confirmed by ^1H NMR spectra to be BNA^+. The structure of the new green compound, **1-Cl**, was revealed by X-ray crystallography (Figure 5). It is surprising that the yield of this product was over 90%. Additionally, we found the reaction between **1-H** and BNA^+ in CH_2Cl_2 releases H_2 identified by GC analysis.

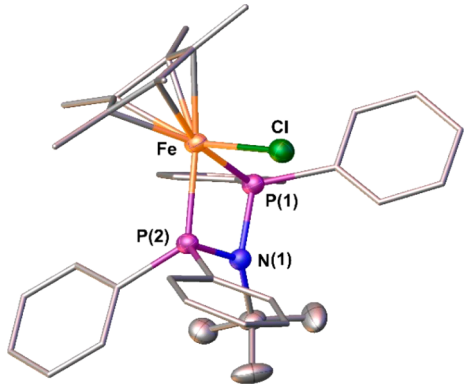

Figure 5. Structure (50% probability thermal ellipsoids) of **1-Cl**. For clarity, the four phenyl groups bound to phosphorus are drawn as lines and hydrogen atoms are omitted. Selected distances (Å) and angles (deg): Fe–P(1) 2.183(2), Fe–P(2) 2.209(2), Fe–Cl 2.318(2), and P(1)–Fe–P(2) 71.75(6).

According to these results, we proposed the reaction pathways shown in eqs 1 and 7–10. The very slow hydride transfer from **1-H** to BNA^+ under the N_2 atmosphere generated a small amount of [**1**-N_2]$^+$ and BNAH.

$$\text{very slow: } [Fe^{II}–H]^0 + BNA^+ + N_2 \rightarrow [Fe^{II}–N_2]^+ + BNAH \quad (1)$$

Once [**1**-N_2]$^+$ produced, it catalyzes the degeneration of **1-H** to **1-Cl** in CH_2Cl_2. Though **1-H** is stable in CH_2Cl_2, the cationic complex [**1**-N_2]$^+$ is highly reactive toward CH_2Cl_2 resulting in formation of ferric complex [**1-Cl**]$^+$ and $C_2H_4Cl_2$ identified by GC-MS analysis (eq 7). Alternatively, the complex [**1-Cl**]$^+$ was prepared by dissolving [**1**-N_2]$^+$ in CH_2Cl_2, and its structure was characterized by X-ray crystallography (Figure 6).

As determined by cyclic voltammograms, the oxidation potential for [**1-Cl**]$^{+/0}$ couple is −0.04 V vs $Fc^{+/0}$, which can oxidize **1-H** ($E_{1/2}^{ox}$ = −0.29 V) producing **1-Cl** and [**1-H**]$^+$ (eq 8). Additionally, [**1-H**]$^+$ are unstable, and undergo H_2 elimination via a disproportionation pathway (eq 9).[3a] Direct evidence is derived from oxidization of **1-H** by $FcBF_4$ in THF, producing H_2 and [**1**-N_2]$^+$ under an N_2 atmosphere.

DOI: 10.1021/acs.organomet.6b00907
Organometallics XXXX, XXX, XXX–XXX

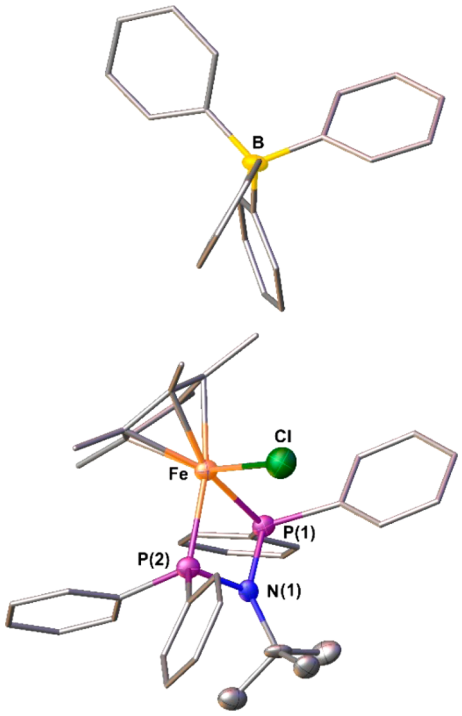

Figure 6. Structure (50% probability thermal ellipsoids) of [**1-Cl**]BPh_4. For clarity, the four phenyl groups bound to phosphorus are drawn as lines and hydrogen atoms are omitted. Selected distances (Å) and angles (deg): Fe−P(1) 2.286(2), Fe−P(2) 2.282(3), Fe−Cl 2.256(2), and P(1)−Fe−P(2) 69.69(8).

$$[Fe^{II}–N_2]^+ + CH_2Cl_2 \rightarrow [Fe^{III}–Cl]^+ + 0.5C_2H_4Cl_2 \quad (7)$$

$$[Fe^{III}–Cl]^+ + [Fe^{II}–H]^0 \rightarrow Fe^{II}–Cl + [Fe^{III}–H]^+ \quad (8)$$

$$[Fe^{III}–H]^+ \rightarrow [Fe^{II}–N_2]^+ + 0.5H_2 \quad (9)$$

Overall, $[Fe^{II}–N_2]^+$ as Catalyst for:

$$[Fe^{II}–H]^0 + CH_2Cl_2 \rightarrow [Fe^{II}–Cl]^0 + 0.5C_2H_4Cl_2 + 0.5H_2 \quad (10)$$

In this way, [**1**-N_2]$^+$ resulting from the hydride transfer from **1-H** to BNA^+ catalyzes the reaction between **1-H** and CH_2Cl_2 (eq 10). Hence, the expected hydride transfer was interrupted.

Hydride Transfer in CH_2Cl_2 in the Presence of MeCN.

Consistent with the results obtained for Cp*(dppe)FeH and Cp*(dppbz)FeH,[10] the stoichiometric reaction of **1-H** with BNA^+ in CD_2Cl_2 in the presence of MeCN produce [**1**(NCMe)]$^+$ and BNAH as both 1,6- and 1,4-isomers (eq 3). Kinetic studies suggest 1,6-BNAH converts to 1,4-BNAH slowly (Figure 7). The rate constant for the reaction of **1-H** with BNA^+ in CD_2Cl_2/CD_3CN (2/1) was determined to be 1.48(9) × 10^{-3} M^{-1} s^{-1} by ^1H NMR at 298 K, which is comparable to 3.2(4) × 10^{-3} M^{-1} s^{-1} for Cp*(dppe)FeH.[10] Although the bite angle ∠P−Fe−P in **1-H** is 2.6° smaller, the hydride transfer rate is 100 times less than that of Cp*(dppm)FeH, which is 1.74(7) × 10^{-1} M^{-1} s^{-1}. That is because Cp*(dppm)FeH has a more electron-rich iron(II) center, reflected by its more negative oxidation potential compared to **1-H**. The results suggest that both electronic and steric factors arising from the chelating diphosphine have influence on the rate of hydride transfer (Figure 8).

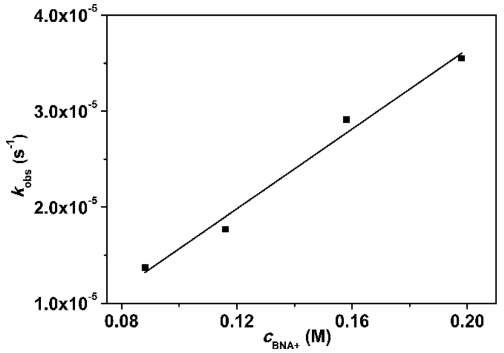

Figure 8. Plot of k_{obs} vs [BNA^+] for the reaction of **1-H** with BNA^+ in C_6D_6/CD_3CN (2/1). Results: k = 2.1(2) × 10^{-4} M^{-1} s^{-1}, R^2 = 0.980.

Hydride Transfer in C_6H_6 in the Presence of MeCN.

Hydride transfer from **1-H** to BNA^+ proceeded in C_6D_6 in the presence of MeCN, and the conversions and product ratios for the stoichiometric reaction in different solvents are shown in Table 1.

The rate constant k for the reaction was determined to be 2.1(2) × 10^{-4} M^{-1} s^{-1} in C_6D_6/CD_3CN (2/1), nearly 10 times faster than that in THF-d_8/CD_3CN (2/1), but much slower compared with that in CD_2Cl_2/CD_3CN (2/1). In the mixed solvents of CD_2Cl_2/MeCN, the ratio of 1,6-/1,4-BNAH

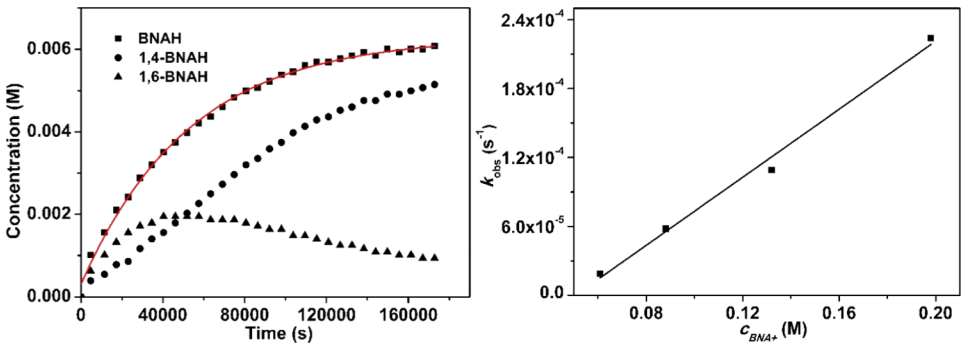

Figure 7. Left, concentrations of BNAH, 1,4-BNAH, and 1,6-BNAH over time detected in the reaction of **1H** and BNA^+ in CD_2Cl_2/CD_3CN (2:1) at 298 K. The initial [**1H**] and [BNA^+] are 6.09 × 10^{-3} M and 6.09 × 10^{-2} M, respectively. Results: k_{obs} = 1.88(5) × 10^{-5} s^{-1}, R^2 = 0.997. Right, plot of k_{obs} vs [BNA^+] for the reaction of **1H** and BNA^+. Results: k = 1.48(9) × 10^{-3} M^{-1} s^{-1}, R^2 = 0.988.

DOI: 10.1021/acs.organomet.6b00907
Organometallics XXXX, XXX, XXX−XXX

Table 1. Product Ratios and the Rate Constants for the Reduction of BNA^+ by 1-H in Different Solvents in the Presence of CD_3CN

	1,6-/1,4-BNAH (yield)[a]		
solvent	24 h	72 h	k (M^{-1} s^{-1})[b]
CD_2Cl_2/MeCN	38:62 (41%)	28:72 (75%)	$1.48(9) \times 10^{-3}$
THF-d_8/MeCN	13:87 (19%)	11:89 (50%)	$1.9(1) \times 10^{-5}$
C_6D_6/MeCN	15:85 (31%)	10:90 (60%)	$2.1(2) \times 10^{-4}$

[a]Conditions: 0.016 mmol of BNA^+, 0.016 mmol **1-H** and 0.16 mmol of CD_3CN in 0.5 mL solvent, room temperature. Product ratios and conversions were determined by ^1H NMR. [b]k was determined in 0.5 mL corresponding solvent and 0.25 mL CD_3CN in the presence of excess BNA^+ (10 equiv).

varied obviously from 38:62 for 24 h to 28:72 for 72 h. These differences observed indicate the solvents indeed influence the hydride transfer process.

CONCLUSIONS

Besides the nucleophilic properties of the metal hydride, the solvent applied has considerable impact on the hydride transfer processes between **1-H** and BNA^+. A coordinative solvent such as MeCN not only acts as the ligand stabilizing the $[Cp^*(Ph_2PN^{tBu}PPh_2)Fe]^+$ fragment to form $[\mathbf{1}(NCMe)]^+$, but also participates in the hydride transfer process. In THF, the hydride transfer proceeds successfully under high pressure of nitrogen, giving the iron(II)−nitrogen complex $[\mathbf{1}\text{-}N_2]^+$ and BNAH. In CH_2Cl_2, the iron(II)−nitrogen complex catalyzes the conversion of **1-H** to **1-Cl**, which interrupts the expected hydride transfer process. Our future work will focus on developing new iron catalysts based on Cp*FeH motif through ligand modification for the reduction of pyridine and its derivatives.

EXPERIMENTAL SECTION

MATERIALS AND METHODS

All reagents were purchased from Sigma-Aldrich, and used as-received. All air-sensitive compounds were prepared and handled using standard Schlenk techniques or in a glovebox under N_2 atmosphere. THF, pentane, Et_2O (dried by distillation over sodium), CH_2Cl_2, and CH_3CN (dried by distillation over CaH_2), for general use were of AR grade and stored under N_2 atmosphere. CD_2Cl_2, CD_3CN, and acetone-d_6 were dried using activated molecular sieves (4 Å) and degassed with three thaw-freeze cycles. C_6D_6 and THF-d_8 were dried over CaH_2 and purified by vacuum transfer. NMR spectra were recorded in a J. Young NMR tube on Bruker Avance 500 spectrometers. ^1H NMR chemical shifts are referenced to the residual proton signal of the deuterated solvent. The ^{31}P NMR spectra were referenced to external H_3PO_4. Single-crystal X-ray diffraction data were collected using a Bruker SMART APEX II diffractometer with a CCD area detector (graphite monochromatic Mo Kα radiation) at 173 K. Infrared spectra were obtained using solid sample on a PerkinElmer FT−IR Spectrometer Spectrum Two in the range of 4000−450 cm^{-1}. Cyclic voltammetry was performed under nitrogen using a CHI 760e electrochemical workstation with a glassy carbon working electrode, a Pt wire counter electrode, and the pseudoreference electrode Ag wire.

N,*N*-bis(diphenylphosphanyl)*tert*-butylamine ($Ph_2PN^{tBu}PPh_2$)[19] and BNA^+ salt[20] were synthesized according to published procedures. $[BNA]PF_6$ and $[BNA]BPh_4$ were prepared by anion exchange in water with NH_4PF_6 or $NaBPh_4$.

$[Cp^*(Ph_2PN^{tBu}PPh_2)Fe(NCMe)]PF_6$. $Ph_2PN^{tBu}PPh_2$ (198 mg, 0.44 mmol) was added at room temperature to a purple solution of $[Cp^*Fe(NCMe)_3]PF_6$ (200 mg, 0.44 mmol) in CH_3CN (40 mL). The color of mixture turned from purple to deep red. After stirring for 3 h, the solvent were removed under vacuum and the residue was extracted with CH_2Cl_2. Recrystallization from CH_2Cl_2/Et_2O afforded $[Cp^*(Ph_2PN^{tBu}PPh_2)Fe(NCMe)]PF_6$ as red microcrystals. Yield: 251 mg, 91%. ^1H NMR (CD_2Cl_2): δ 8.10−8.08 (m, 4H, C_6H_5), 7.67−7.65 (m, 6H, C_6H_5), 7.56−7.53 (m, 10H, C_6H_5), 1.45 (s, 3H, FeNCCH_3), 1.34 (s, 15H, Cp*), 0.86 (s, 9H, CH_3). ^{31}P NMR (CD_2Cl_2): δ 126.8. ESI-MS: calcd for $[Cp^*(Ph_2PN^{tBu}PPh_2)Fe]^+$ 632.2298; found: 632.2443. Anal. Calcd. for $C_{40}H_{47}F_6FeN_2P_3$: C, 58.69; H, 5.79; N, 3.42. Found: C, 58.92; H, 5.53; N, 3.21.

$Cp^*(Ph_2PN^{tBu}PPh_2)FeH$. $NaBH_4$ (26 mg, 0.684 mmol) was added to a THF solution of $[Cp^*(Ph_2PN^{tBu}PPh_2)Fe(NCMe)]PF_6$ (280 mg, 0.342 mmol) at −30 °C. The temperature was raised to room temperature over a period of 3 h, and the color of the solution turned orange. The solvent was removed under vacuum leaving a gummy residue which was extracted with pentane. The product was recrystallized from pentane and isolated by filtration to give the product as red solid. Yield: 170 mg, 78%. ^1H NMR (C_6D_6): δ 8.48−8.42 (q, 4H, C_6H_5), 8.15−8.10 (q, 4H, C_6H_5), 7.29−7.10 (m, 12H, C_6H_5), 1.61 (s, 15H, Cp*), 0.79 (s, 9H, CH_3), −13.55 (t, 1H, J_{P-H} = 63 Hz, Fe—H). ^{31}P NMR (C_6D_6): δ 129.6. Anal. Calcd. for $C_{38}H_{45}FeNP_2$: C, 75.83; H, 7.16; N, 2.21. Found: C, 75.58; H, 7.34; N, 2.13. IR (solid, ν_{Fe-H}): 1908 cm^{-1}.

Scaled-Up Reaction of $Cp^*(Ph_2PN^{tBu}PPh_2)FeH$ and BNA^+ in THF under 60 psi N_2. **1-H** (60 mg, 0.095 mmol) and $[BNA]BPh_4$ (52 mg, 0.095 mmol) were combined in a Fischer−Porter bottle under an N_2 atmosphere. Then 5 mL THF was added, and the resulting solution was stirred under 60 psi of N_2 for 48 h. The solvent was removed under vacuum, and the residue was washed with toluene three times to remove the resulting BNAH. The mixture was redissolved in THF and filtered through a short pad of diatomaceous earth. The solution was concentrated to 3 mL, layered with hexane and placed at −30 °C for 24 h to give $[Cp^*(Ph_2PN^{tBu}PPh_2)Fe(N_2)]BPh_4$ as red solid. Yield: 38 mg, 41%. ^1H NMR (acetone-d_6): δ 8.22 (m, 4H, C_6H_5), 7.90−7.85 (m, 4H, C_6H_5), 7.70−7.67 (m, 4H, C_6H_5), 7.34 (m, 10H, C_6H_5), 6.93−6.90 (m, 12H, C_6H_5), 6.78−6.76 (m, 6H, C_6H_5), 1.51 (s, 15H, Cp*), 1.0 (s, 9H, CH_3). ^{31}P NMR (acetone-d_6): δ 116.2. Anal. Calcd. for $C_{62}H_{64}BFeN_3P_2$: C, 76.00; H, 6.58; N, 4.29. Found: C, 75.63; H, 6.23; N, 4.17. IR (solid, ν_{NN}): 2132 cm^{-1}.

$Cp^*(Ph_2PN^{tBu}PPh_2)FeCl$. **1-H** (50 mg, 0.079 mmol) and $[BNA]BPh_4$ (42 mg, 0.079 mmol) were combined in 10 mL CH_2Cl_2 under an N_2 atmosphere. The mixture was stirred at room temperature for 36 h, after which the solvent was removed in vacuo, and the residue was extracted with hexane. The solution was concentrated to 2 mL in vacuo and placed under −30 °C for 24 h to give the product as dark green solid. Yield: 48 mg, 91%. Anal. Calcd. for $C_{38}H_{44}ClFeNP_2$: C, 68.32; H, 6.64; N, 2.10. Found: C, 68.57; H, 6.33; N, 2.56.

$[Cp^*(Ph_2PN^{tBu}PPh_2)FeCl]BPh_4$. The initial orange solution gradually turned to deep brown when 1 mL CH_2Cl_2 was added to the THF solution of $[\mathbf{1}\text{-}N_2]BPh_4$ (20 mg, 0.02

DOI: 10.1021/acs.organomet.6b00907
Organometallics XXXX, XXX, XXX−XXX

mmol). The mixture was stirred at room temperature for 12 h and red crystals were isolated upon concentration and layered with hexane. Yield: 15.2 mg, 77%. ESI−MS calcd for $[Cp^*(Ph_2PN^{tBu}PPh_2)FeCl]^+$: 667.1987; found: 667.1993. Anal. Calcd. for $C_{62}H_{64}ClFeNP_2$: C, 75.43; H, 6.53; N, 1.42. Found: C, 75.15; H, 6.28; N, 1.31.

$[Cp^*(Ph_2PN^{tBu}PPh_2)FeCO]BPh_4$. CO was bubbled through a 10 mL THF solution of $[1\text{-}N_2]BPh_4$ (30 mg, 0.03 mmol). The solution was stirred for 30 min, during which time the color turned from orange to light green. After filtration through diatomaceous earth, the mixture was concentrated to 5 mL in vacuum. Then 20 mL hexane was added to precipitate the product as a light green solid. Yield: 22 mg, 75%. ^{1}H NMR (acetone-d_6): δ 8.23−8.20 (m, 4H, C_6H_5), 7.87−7.83 (m, 10H, C_6H_5), 7.68−7.64 (m, 6H, C_6H_5), 7.36−7.32 (m, 8H, C_6H_5), 6.94−6.89 (m, 8H, C_6H_5), 6.79−6.77 (m, 4H, C_6H_5), 1.63 (s, 15H, Cp*), 0.97 (s, 9H, CH_3). ^{31}P NMR (acetone-d_6): δ 111.3. Anal. Calcd. for $C_{63}H_{64}BFeNOP_2$: C, 77.23; H, 6.58; N, 1.43; O, 1.63. Found: C, 77.62; H, 6.38; N, 1.25; O, 1.29. IR (solid, ν_{CO}): 1969 cm^{-1}.

NMR Measurements of Rate Constants for Hydride Transfer from $Cp^*(Ph_2PN^{tBu}PPh_2)FeH$ to BNA^+. In a typical experiment, **1-H** (4.2 mg, 0.0066 mmol) and $[BNA]PF_6$ (23.7 mg, 0.066 mmol) were placed in a vial under a nitrogen atmosphere in a glovebox. CD_2Cl_2 (0.5 mL) and CD_3CN (0.25 mL) were added by gastight syringe, and the solution was immediately transferred to a J. Young NMR tube. The first ^{1}H NMR spectrum was recorded within 5 min, and then single-pulse spectra were taken every 300 s until the completion of the reaction. The integral values of the CH_2 of the benzyl group corresponding to 1,4-BNAH (4.21 ppm) and 1,6-BNAH (4.14 ppm) were compared to that of residual diethyl ether (m, 3.317−3.386 ppm).

■ ASSOCIATED CONTENT

Supporting Information

The Supporting Information is available free of charge on the ACS Publications website at DOI: 10.1021/acs.organomet.6b00907.

Experimental details, NMR (^{1}H, ^{31}P), and IR spectra- (PDF)

Crystallographic data (CIF)

■ AUTHOR INFORMATION

Corresponding Author

*E-mail: wwg@sdu.edu.cn (W.W.).

ORCID

Chen-Ho Tung: 0000-0001-9999-9755

Wenguang Wang: 0000-0002-4108-7865

Notes

The authors declare no competing financial interest.

■ ACKNOWLEDGMENTS

We gratefully acknowledge the financial support from the "1000 Youth Talents Plan", the Natural Science Foundation of China and Shandong Province (21402107, 91427303, and ZR2014M011). We also thank Prof. Di Sun for assistance with the X-ray crystallography.

■ REFERENCES

(1) Murakami, Y.; Kikuchi, J.-i.; Hisaeda, Y.; Hayashida, O. *Chem. Rev.* **1996**, *96*, 721.

(2) Bull, J. A.; Mousseau, J. J.; Pelletier, G.; Charette, A. B. *Chem. Rev.* **2012**, *112*, 2642.

(3) (a) Hu, Y.; Shaw, A. P.; Estes, D. P.; Norton, J. R. *Chem. Rev.* **2016**, *116*, 8427. (b) Fukuzumi, S.; Suenobu, T. *Dalton. Trans.* **2013**, *42*, 18. (c) McSkimming, A.; Colbran, S. B. *Chem. Soc. Rev.* **2013**, *42*, 5439.

(4) (a) Paul, C. E.; Arends, I. W. C. E.; Hollmann, F. *ACS Catal.* **2014**, *4*, 788. (b) Quinto, T.; Köhler, V.; Ward, T. R. *Top. Catal.* **2014**, *57*, 321. (c) Okamoto, Y.; Köhler, V.; Paul, C. E.; Hollmann, F.; Ward, T. R. *ACS Catal.* **2016**, *6*, 3553. (d) Zheng, C.; You, S.-L. *Chem. Soc. Rev.* **2012**, *41*, 2498. (e) Prier, C. K.; Rankic, D. A.; MacMillan, D. W. *Chem. Rev.* **2013**, *113*, 5322.

(5) (a) Lo, H. C.; Buriez, O.; Kerr, J. B.; Fish, R. H. *Angew. Chem., Int. Ed.* **1999**, *38*, 1429. (b) Lo, H. C.; Leiva, C.; Buriez, O.; Kerr, J. B.; Olmstead, M. M.; Fish, R. H. *Inorg. Chem.* **2001**, *40*, 6705. (c) Hu, Y.; Li, L.; Shaw, A. P.; Norton, J. R.; Sattler, W.; Rong, Y. *Organometallics* **2012**, *31*, 5058.

(6) Barrett, S. M.; Pitman, C. L.; Walden, A. G.; Miller, A. J. *J. Am. Chem. Soc.* **2014**, *136*, 14718.

(7) (a) Koga, K.; Matsubara, Y.; Kosaka, T.; Koike, K.; Morimoto, T.; Ishitani, O. *Organometallics* **2015**, *34*, 5530. (b) Matsubara, Y.; Kosaka, T.; Koga, K.; Nagasawa, A.; Kobayashi, A.; Konno, H.; Creutz, C.; Sakamoto, K.; Ishitani, O. *Organometallics* **2013**, *32*, 6162. (c) Soldevila-Barreda, J. J.; Bruijnincx, P. C. A.; Habtemariam, A.; Clarkson, G. J.; Deeth, R. J.; Sadler, P. J. *Organometallics* **2012**, *31*, 5958. (d) Kobayashi, A.; Takatori, R.; Kikuchi, I.; Konno, H.; Sakamoto, K.; Ishitani, O. *Organometallics* **2001**, *20*, 3361.

(8) (a) Guan, H.; Iimura, M.; Magee, M. P.; Norton, J. R.; Zhu, G. *J. Am. Chem. Soc.* **2005**, *127*, 7805. (b) Guan, H.; Iimura, M.; Magee, M. P.; Norton, J. R.; Janak, K. E. *Organometallics* **2003**, *22*, 4084.

(9) Shaw, A. P.; Ryland, B. L.; Franklin, M. J.; Norton, J. R.; Chen, J. Y.-C.; Hall, M. L. *J. Org. Chem.* **2008**, *73*, 9668.

(10) Zhang, F.; Jia, J.; Dong, S.; Wang, W.; Tung, C.-H. *Organometallics* **2016**, *35*, 1151.

(11) Cheng, J.-P.; Lu, Y.; Zhu, X.; Mu, L. *J. Org. Chem.* **1998**, *63*, 6108.

(12) Hamon, P.; Toupet, L.; Hamon, J.-R.; Lapinte, C. *Organometallics* **1996**, *15*, 10.

(13) Giannoccaro, P.; Rossi, M.; Sacco, A. *Coord. Chem. Rev.* **1972**, *8*, 77.

(14) Sellmann, D.; Kleinschmidt, E. *J. Organomet. Chem.* **1977**, *140*, 211.

(15) Crossland, J. L.; Tyler, D. R. *Coord. Chem. Rev.* **2010**, *254*, 1883.

(16) Leal, A. d. l. J.; Tenorio, M. J.; Puerta, M. C.; Valerga, P. *Organometallics* **1995**, *14*, 3839.

(17) Hu, Y.; Norton, J. R. *J. Am. Chem. Soc.* **2014**, *136*, 5938.

(18) Cheng, T.-Y.; Bullock, R. M. *Organometallics* **2002**, *21*, 2325.

(19) Maumela, M.; Blann, K.; de Bod, H.; Dixon, J.; Gabrielli, W.; Williams, D. B. *Synthesis* **2007**, *2007*, 3863.

(20) (a) Paul, C. E.; Gargiulo, S.; Opperman, D. J.; Lavandera, I.; Gotor-Fernandez, V.; Gotor, V.; Taglieber, A.; Arends, I. W. C. E.; Hollmann, F. *Org. Lett.* **2013**, *15*, 180. (b) Zhu, X.-Q.; Tan, Y.; Cao, C.-T. *J. Phys. Chem. B* **2010**, *114*, 2058.

DOI: 10.1021/acs.organomet.6b00907
Organometallics XXXX, XXX, XXX−XXX